

APPLIED ECOLOGY

Robust estimates of a high N_e/N ratio in a top marine predator, southern bluefin tunaRobin S. Waples^{1*}, Peter M. Grewe², Mark W. Bravington², Richard Hillary², Pierre Feutry²

Genetic studies of several marine species with high fecundity have produced “tiny” estimates ($\leq 10^{-3}$) of the ratio of effective population size (N_e) to adult census size (N), suggesting that even very large populations might be at genetic risk. A recent study using close-kin mark-recapture methods estimated adult abundance at $N \approx 2 \times 10^6$ for southern bluefin tuna (SBT), a highly fecund top predator that supports a lucrative (~\$1 billion/year) fishery. We used the same genetic and life history data (almost 13,000 fish collected over 5 years) to generate genetic and demographic estimates of N_e per generation and N_b (effective number of breeders) per year and the N_e/N ratio. Demographic estimates, which accounted for age-specific vital rates, skip breeding, variation in fecundity at age, and persistent individual differences in reproductive success, suggest that N_e/N is >0.1 and perhaps about 0.5. The genetic estimates supported this conclusion. Simulations using true $N_e = 5 \times 10^5$ ($N_e/N = 0.25$) produced results statistically consistent with the empirical genetic estimates, whereas simulations using $N_e = 2 \times 10^4$ ($N_e/N = 0.01$) did not. Our results show that robust estimates of N_e and N_e/N can be obtained for large populations, provided sufficiently large numbers of individuals and genetic markers are used and temporal replication (here, 5 years of adult and juvenile samples) is sufficient to provide a distribution of estimates. The high estimated N_e/N ratio in SBT is encouraging and suggests that the species will not be compromised by a lack of genetic diversity in responding to environmental change and harvest.

INTRODUCTION

Effective population size (N_e) is the evolutionary analog of census size (N). Whereas census size strongly influences rates of demographic/ecological processes like competition, predation, and population growth rates, N_e controls the rates of inbreeding, genetic drift, and loss of genetic diversity and influences effectiveness of natural selection (1). Because effective size is challenging to estimate in natural populations, considerable interest has focused on the ratio of effective size to census size, N_e/N (2, 3). If specific N_e/N values consistently apply to certain classes of species, then information about abundance could be used to predict rates of evolutionary processes at the population level. However, although considerable theoretical and empirical efforts have been made to find relationships between N_e/N and a variety of life history features (4–7), a completely general framework remains elusive.

Two factors in particular make this challenging. First, a number of studies have found a negative correlation between N_e/N and N . Possible explanations for this pattern include reduced variance in reproductive success at low abundance (8, 9), increased adult mortality that reduces N more than N_e (10), and density-dependent effects that increase offspring survival and generation length at low density (11). However, the major point of controversy about N_e/N ratios involves the hypothesis of sweepstakes reproductive success (SRS) in marine species (12, 13), which postulates that N_e/N could be tiny ($\leq 10^{-3}$) in species with high fecundity, if only a few families “win the sweepstakes” by producing offspring that survive to reproduce. Numerous estimates of N_e/N in the range 10^{-3} to 10^{-6} have been published for high-fecundity marine species (13, 14). If the N_e/N ratio is this small, it is important to know because even very large populations ($N \geq 10^6$) could be at genetic risk. Some authors (15) argue that these concerns potentially apply quite generally to marine species with high fecundity.

Here, we evaluate the possibility of a tiny N_e/N ratio in southern bluefin tuna (SBT; *Thunnus maccoyii*), a large, mobile, top marine predator with broadcast spawning and high batch fecundity ($>6 \times 10^6$)—life history traits that are often associated with SRS. SBT support an important international fishery, the value of which has been estimated at $> \$1$ billion/year; the species is also generally considered highly depleted, but traditional methods (such as traditional mark-recapture) have not been able to provide reliable estimates of stock status or recovery probability (16). For these reasons (high value + high uncertainty), SBT were targeted for the first large-scale application of close-kin mark-recapture (CKMR) methods to estimate abundance (16). This project sampled almost 13,000 juveniles and adults over 5 years (Table 1) and produced an estimate of adult population size ($N \approx 2 \times 10^6$) that was both higher and more precise [coefficient of variation (CV) = 0.17] than previous methods allowed. With this estimate of census size as a reference point, we used the extensive array of CKMR samples, together with life history information for SBT, to generate both genetic and demographic estimates of effective size, as well as the N_e/N ratio. We also simulated genetic data for two effective sizes corresponding to N_e/N ratios of 0.25

Table 1. Sample sizes used in the genetic analyses. Values in parentheses are harmonic mean numbers of individuals actually used over all pairwise comparisons of loci.

Year	Adults	Juveniles
2006	212 (205)	1497 (1285)
2007	1409 (1073)	1625 (1187)
2008	1466 (878)	1408 (737)
2009	1379 (1018)	1316 (1240)
2010	1160 (1112)	1405 (1324)
Total	5626 (4286)	7251 (5773)

¹Northwest Fisheries Science Center, National Marine Fisheries Service, National Oceanic and Atmospheric Administration, Seattle, WA 98112, USA. ²Commonwealth Scientific and Industrial Research Organisation (CSIRO) Oceans and Atmosphere, G.P.O. Box 1538, Hobart 7001, Tasmania, Australia.

*Corresponding author. Email: robin.waples@noaa.gov

and 0.01 to compare with the empirical genetic estimates. Results of our demographic and genetic analyses are congruent and reject the possibility of tiny N_e/N in SBT. Instead, our results suggest that N_e/N is > 0.1 and perhaps about 0.5.

RESULTS

Population demography

The demographic model for SBT uses discrete time periods in years, indexed by x . Reproduction occurs in Indonesia and follows the seasonal birth-pulse model (17). At age x , each individual produces an average of b_x offspring and then survives to age $x + 1$ with probability s_x . Available data were sufficient only for a single estimate of constant adult survival for both sexes [$s_x = 0.77/\text{year}$; (16)]. Age at maturity (α) was fixed at age 8, maximum age was set to 30, and population size was $N = 1.97 \times 10^6$ adults [(16); see Materials and Methods]. Age-specific vital rates for SBT used in the analyses below are shown in table S1.

Compared to some other marine ectotherms, male SBT have a less pronounced increase in fecundity with age, while females show a strongly sigmoidal pattern owing to increases in per-kilo reproductive success of older females (Fig. 1). The combination of delayed maturity and increasing fecundity with age leads to a relatively long generation time ($T = \text{mean age of parents} = 13.3$ years). Because of the steeper increase in fecundity with age, generation length is longer for females (14.7 years) than for males (11.9 years).

Demographic estimates of effective size

For iteroparous species like SBT, it is important to distinguish two kinds of effective size: N_e is the effective population size per generation, and N_b is the effective number of breeders per year or breeding cycle. N_e determines the rates of evolutionary processes (such as genetic drift and loss of genetic variability) in the population as a whole, but N_b is often easier to estimate and provides important insights into the breeding system and reproductive dynamics.

We used the program AgeNe (18) to produce demographic estimates of N_e and N_b based on SBT vital rates. In addition to age-specific

estimates of survival and fecundity, calculation of N_e requires a third vital rate: $\phi_x = V_{k(x)}/b_x$, which is the ratio of the variance to the mean reproductive success in one time period for individuals of age x . Random variation in reproductive success among same-age, same-sex individuals produces $\phi_x \approx 1$. We calculated N_e per generation using Hill’s (19) formula

$$N_e = \frac{4N_1 T}{V_{k^*} + 2} \tag{1}$$

where N_1 is the number of offspring produced each time period that reach age at recruitment, and V_{k^*} is lifetime variance in reproductive success (production of offspring) among the N_1 individuals in a cohort. For SBT, $N_1 = 4.54 \times 10^5$ recruits/year produces an adult population size of 1.97×10^6 , which is similar to the estimate from the CKMR study (16). N_b is calculated using the standard discrete-generation formula for inbreeding effective size (20)

$$N_b = \frac{\bar{k}N - 2}{\bar{k} - 1 + V_k/\bar{k}} \tag{2}$$

where N is adult census size and V_k and \bar{k} are computed across both sexes on the basis of offspring produced in a single reproductive cycle. In contrast to the age-specific values of $\phi_x = V_{k(x)}/b_x$ described above, V_k and \bar{k} in Eq. 2 apply to individuals of all ages that reproduce in one time period.

Empirical data for ϕ_x are rarely available for natural populations, but for SBT, we were able to use empirical data on variance of fecundity at age (table S2) to estimate ϕ_x . This analysis considers a variation of the original Wright-Fisher model in which individuals contribute unequally to a very large gamete pool from which the next cohort of offspring is randomly drawn. Our analyses showed that, assuming random survival of fertilized eggs until recruitment, the observed variance in fecundity at age would have only a trivial effect ($\phi_x < 1.02$ for all ages in both males and females; table S2). These should be considered minimal estimates of ϕ_x because they only account for effects of body size and not other factors (for example, behavior and physiology) that can affect reproductive output.

A useful point of reference for evaluating the N_e/N ratio is an “ideal” Wright-Fisher population with discrete generations, in which $N_e = N_b = N$ (ideal scenario in Fig. 2). The other scenarios in this figure all use the SBT vital rates in table S1, with modifications or additions as noted on the figure, and scale population size to produce a constant $N = 1.97 \times 10^6$ adults age 8 and older. Using the empirical SBT vital rates, including the minimum estimates of ϕ_x , initial demographic estimates of effective size are 1.34×10^6 for N_b and 1.86×10^6 for N_e , with the latter producing a high estimated N_e/N ratio of 0.93 (Fig. 2). This estimate, which is not much below the 1.0 ratio for an ideal population, reflects combined effects of three major life history traits.

First, discrete-generation populations reproduce in a single year or season, whereas SBT have adult life spans of up to 23 years. In the “ $\alpha = 1$, fixed b_x ” scenario in Fig. 2, the population matures at age 1 and fecundity is invariant with age (both as in the discrete generation model), but annual adult survival, adult life span, and ϕ_x use the SBT values from table S1. Under these conditions, N_e/N drops to 0.56. This decline reflects the fact that, in iteroparous species, by chance some individuals live longer than others and reproduce more times; this increases lifetime variance in reproductive success ($V_{k(x)}$) and reduces N_e/N compared to

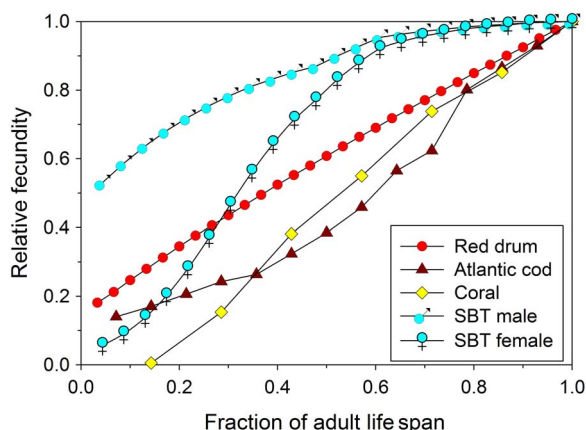


Fig. 1. Change in fecundity with age. The y axis shows fecundity relative to the maximum for the specified species and sex. Data for male and female SBT are compared to female data for some other marine ectotherms. Data for red drum (*Sciaenops ocellatus*), Atlantic cod (*Gadus morhua*), and the solitary coral (*Balanophyllia elegans*) are from (7). These species all have life history traits (high fecundity and broadcast spawning) typical of species that exhibit SRS, and some authors have reported tiny estimates of N_e/N for red drum and cod (14).

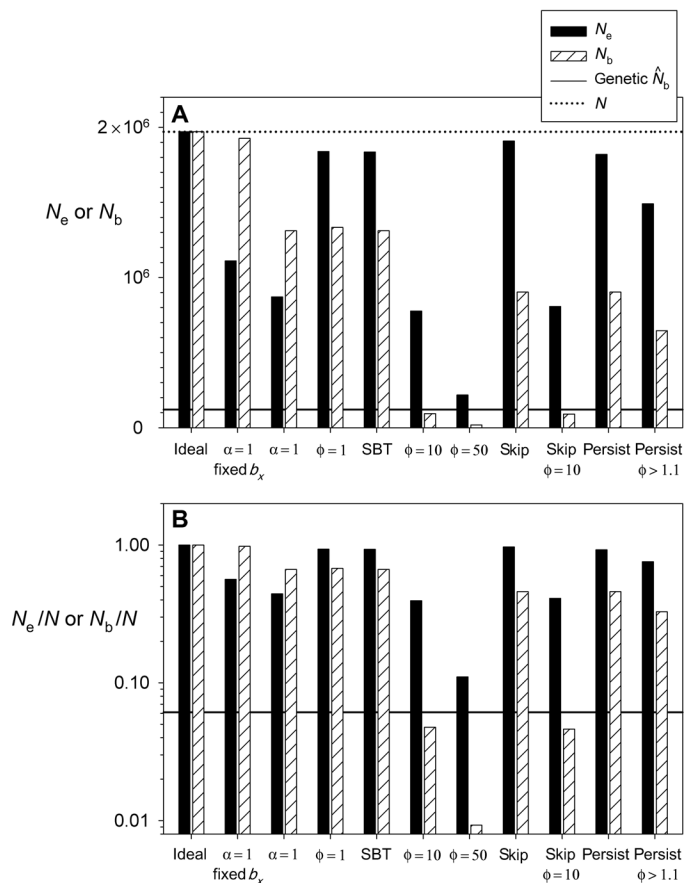


Fig. 2. Effects of life history traits on effective population size. Shown are demographic estimates of annual and generational effective size (A) and the effective size/census size ratio (B; note the log scale on the y axis). The ideal scenario represents a Wright-Fisher population with discrete generations. The “SBT” scenario used empirical age-specific vital rates from table S1; the other scenarios used the same data except as noted. Variations considered included earlier age at maturity ($\alpha = 1$), constant fecundity with age (“fixed b_x ”), different assumed values of $\phi =$ the ratio of variance to mean reproductive success among individuals of the same age and sex, and whether effects of skip breeding (“skip”) or persistent individual differences (“persist”) were considered. In all scenarios, adult census size [dotted line in (A)] was $N = 1.97 \times 10^6$. The solid horizontal lines show the combined (weighted harmonic mean across years) genetic estimate of N_b (A) or N_b/N (B) using $P_{crit} = 0.01$. Data for this figure are shown in table S3.

the discrete-generation model, where all individuals die at the same age. Results for the $\alpha = 1$, fixed b_x scenario are consistent with previous work (4, 6), which has shown that, with constant vital rates, $\alpha = 1$, and all $\phi = 1$, N_e/N converges on 0.5 as adult life span increases. Alternative scenarios that used higher or lower estimates of adult survival did not appreciably affect the results (Supplementary Methods; table S3).

The second major factor that reduces N_e/N in SBT is age-related changes in fecundity. When fecundity increases with age, as it does in both sexes in SBT (Fig. 1), individuals that live longer not only get to reproduce more often, their output also goes up each year. This further exacerbates disparities in lifetime reproductive success and reduces N_e/N . In the “ $\alpha = 1$ ” scenario, adding the SBT vital rates for fecundity further dropped N_e/N to 0.44, an additional decline of 22%.

Compensating for these two negative factors is a third factor that substantially increases N_e/N : SBT do not mature until age 8. Delayed maturity increases generation length, and because T appears in the

numerator of Eq. 1, N_e also increases proportionally. The only difference between the SBT and the $\alpha = 1$ scenarios is the delayed age at maturity in SBT, which more than doubles N_e/N (from 0.44 to 0.93). Compared to these major life history effects, the very slight increase in ϕ based on empirical fecundity at age data reduces N_e only trivially (0.1%) from what it would be under random reproductive success (compare results for “ $\phi = 1$ ” and SBT scenarios in Fig. 2).

Because the minimum estimates of ϕ do not capture all factors that can influence variation in reproductive success—including family-correlated survivals that could be important for highly fecund species—we also estimated N_e and N_b assuming higher fixed values of ϕ ranging from 10 to 10^4 . N_e/N drops to 0.39 for $\phi = 10$ and to 0.11 for $\phi = 50$ (Fig. 2), and subsequently drops by an order of magnitude for each order of magnitude increase in ϕ (fig. S1). Only for the extreme scenario with $\phi = 10^4$ does the estimated effective size/census size ratio drop to the range of tiny estimates that have appeared in the literature [$N_e/N \leq 10^{-3}$; (14, 21)]. $\phi = 10^4$ requires that only 1 in about 10^3 to 10^4 adults successfully reproduces each year (21). N_b is more sensitive than N_e to high values of ϕ ; whereas increasing ϕ from near 1 to 10 drops N_e/N by 58%, it causes a decline of 93% in N_b/N , to 0.05.

Other important factors that can influence both N_e and N_b are skip breeding and persistent individual differences in reproductive success. Assuming that only half of SBT aged 8 to 12 are available to spawn in a given year (see Materials and Methods), annual N_b would be reduced by about 31% to 9.0×10^5 (skip scenario; Fig. 2 and table S3). This reduction is fairly large because young fish make up a substantial fraction of the adult population. Skip breeding has a proportionally smaller effect on N_b if ϕ is assumed to be higher (the reduction is only about 4% for $\phi = 10$; table S3). Conversely, N_e per generation increases with skip breeding because it helps ensure that different parents get to reproduce in different years. Because only part of the adult population is affected, we estimated the increase in N_e at only 4%, which is at the lower end of the range reported for species with high fecundity and high juvenile mortality (22).

If some individuals are consistently (across multiple time periods) good or bad at producing offspring, this consistency has no effect on N_b per year but reduces N_e per generation, because it increases variation among individuals in lifetime reproductive success. When we modeled persistent differences in reproductive success by assuming they scaled directly with empirical estimates of the CV of fecundity at age, we found a negligible (1%) effect on N_e (compare SBT and persist scenarios in Fig. 2). However, if the CV of fecundity at age were assumed to be five times as large as the empirical estimate (leading to a modest increase in ϕ to 1.1 to 1.4), N_e would decline by 18% (“persist, $\phi > 1.1$ ” scenario). This shows that fairly small increases in ϕ , if they are persistent over time, can substantially influence effective population size.

Genetic estimates of effective size

The 25 microsatellite loci used here were developed specifically for SBT to determine parentage among a set of adult and juveniles sampled from the wild fishery (16, 23). The loci were chosen to be highly polymorphic and easily scored. The genetic estimates of effective size reflect quantitative adjustments to account for both physical linkage and effects of age structure. Results reported here include sensitivity analyses of effects of removing two loci with estimated frequencies of null alleles $>10\%$ and use of two criteria for screening out rare alleles.

Estimates of yearly N_b

The 10 adjusted point estimates of N_b from yearly juvenile samples were all $>10^4$, and 3 were infinitely large [indicating that all of the observed

linkage disequilibrium (LD) could be explained by sampling error; Figs. 3 and 4). Lower bounds for all 95% confidence intervals (CIs) were also $>10^4$. The combined (across years) estimates were 7.9×10^4 to 1.2×10^5 , which produce estimates of the N_b/N ratio of 0.04 to 0.06 (table S3).

Estimates of generational N_e

Adjusted point estimates of N_e for 2006 and 2007 were between 10^4 and 10^5 , while those for the last 3 years (2008–2010) were all infinite (Fig. 3). The 2006 sample included only 212 adults (Table 1; more than 1100 were sampled every other year), and the 2006 adult N_e estimates were also the only ones for which the lower bound of the 95% CIs dipped below 10^4 . Combined estimates computed across all 5 years of adult samples were infinitely large, with a lower 95% confidence bound

of $\sim 2 \times 10^4$. The annual point estimates of N_e shown in Fig. 3 translate into N_e/N values that were either indeterminate (when estimated $N_e = \infty$) or fell in the range 0.01 to 0.1.

Simulated data

The two simulated scenarios used amounts of data comparable to those available for SBT, with effective sizes of $N_e = 5 \times 10^5$ (close to the demographic estimate assuming $\phi = 10$) and $N_e = 2 \times 10^4$ (which would produce an N_e/N ratio of 0.01—a reduction of 99% from the adult census size). The distribution of simulated estimates for $N_e = 5 \times 10^5$ closely resembled, and were not statistically different from ($P > 0.1$), the empirical estimates of effective size in SBT: No point estimates were below 10^4 , most finite estimates fell between 10^4 and 10^6 , and a substantial fraction of estimates were infinitely large (Fig. 4). In contrast, when the smaller N_e was simulated, 100% of the point estimates fell between 11,000 and 67,000, and this tight distribution was statistically incompatible with empirical data for both N_b and N_e ($P < 10^{-6}$). Thus, if true N_e were as small as 2×10^4 , we would not expect to see any appreciable fraction of infinite estimates—which is at odds with the pattern actually observed for SBT.

Statistical theory provides an additional perspective for evaluating the empirical and simulated estimates of effective size. Expected

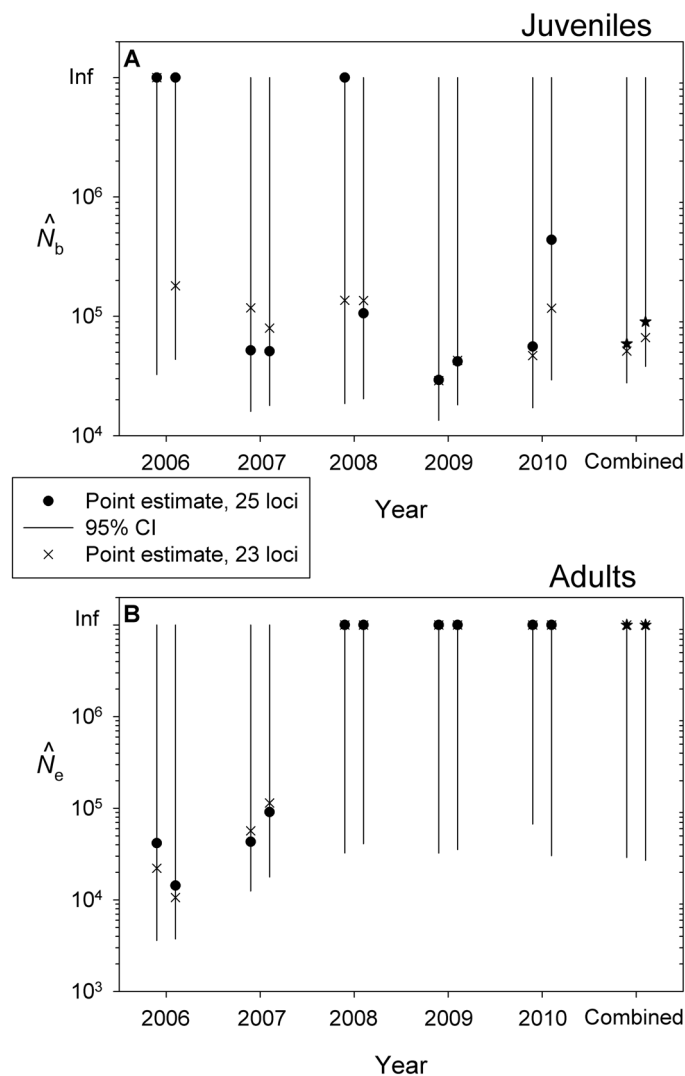


Fig. 3. CIs for genetic estimates of effective population size. Estimates of N_b from juveniles (A) and N_e from adults (B) for 5 years of genetic samples. Filled circles are point estimates using 25 loci; \times denotes estimates after dropping two loci with $>10\%$ estimated null allele frequency. Vertical lines are 95% CIs for 25 locus estimates. All upper bounds for CIs are infinity. For each sample year, results on the left screen out alleles with frequency <0.02 , and results on the right screen out alleles with frequency <0.01 . “Combined” estimates are weighted harmonic means across the 5 years. All estimates used the LD method adjusted to account for effects of age structure (25) and physical linkage (26).

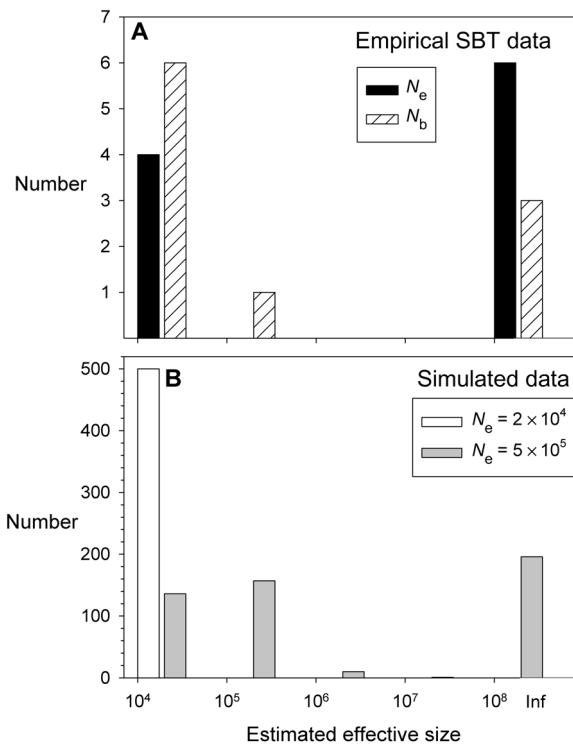


Fig. 4. Distribution of genetic estimates of effective population size. (A) Empirical estimates for SBT. Each data point represents 1 year of juvenile samples (which estimate N_b ; striped bars) or adult samples (which estimate N_e ; black bars). These results include data for both $P_{crit} = 0.01$ and 0.02 (see Fig. 3 for CIs for point estimates). (B) Estimates of N_e based on samples from 500 simulated populations with discrete generations and true $N_e = 2 \times 10^4$ (white bar) or 5×10^5 (gray bars). Each simulated sample included 1500 individuals scored for 350 diallelic (“SNP”) loci. Empirical distributions of both N_b and N_e were not statistically different from the distribution of simulated estimates for $N_e = 5 \times 10^5$ ($P > 0.1$, two-sample Kolmogorov-Smirnov test), but both empirical distributions were incompatible with the distribution of simulated estimates for $N_e = 2 \times 10^4$ ($P < 10^{-6}$).

precision of the LD method can be evaluated using the following equation (24)

$$CV(\hat{N}_e) \approx \sqrt{2/n} \left[1 + \frac{3N_e}{s} \right]$$

where n is the number of pairwise comparisons of alleles and S is the number of individuals sampled. Substituting for $n = 350(349)/2 = 61,075$ and $S = 1500$ to approximate the amount of data available for SBT (see Materials and Methods) produces

$$CV(\hat{N}_e) \approx \sqrt{2/61,075} \left[1 + \frac{N_e}{500} \right] = 0.0057 \left[1 + \frac{N_e}{500} \right]$$

For the two simulation scenarios, expected CVs for \hat{N}_e are 0.24 for $N_e = 2 \times 10^4$ and 5.7 for $N_e = 5 \times 10^5$. This result shows that relatively precise estimates of effective size can be made even in relatively large populations, provided a sufficient number of genetic markers are available and the ratio N_e/S is not too large; we confirmed this in the simulations using $N_e = 2 \times 10^4$. However, this also illustrates the difficulty in obtaining precise estimates of effective size when true N_e is orders of magnitude larger than the sample size, as is the case for the larger simulated effective size. In that case, replication across multiple samples (for SBT, five samples each were available for juveniles and adults) can be very valuable to allow comparison of distributions rather than individual point estimates.

DISCUSSION

The CKMR study for SBT (16) obtained a robust estimate of adult abundance that was both higher and much more precise than had been possible with other methods. Here, we have used the same genetic data from the same juvenile and adult samples, together with the life history information for SBT that informed the CKMR estimates of abundance, to generate both genetic and demographic estimates of effective population size (N_e per generation and N_b per year). In addition, directly comparing the new data with the CKMR results has allowed us to produce robust estimates of the effective size/census size ratio. Our results illustrate the synergistic benefits of jointly considering demographic and genetic data to study evolutionary processes in large populations. The two approaches have different statistical properties that complement each other to produce robust estimates. The demographic approaches start with an upper limit of $N_e/N \approx 1$ and consider various factors that could lower the ratio. However, demographic data generally provide only indirect information about the key age-specific parameter ϕ . If ϕ is very high, N_e/N could be very low, or even in the tiny range ($\leq 10^{-3}$). Conversely, genetic methods struggle to distinguish very large N_e from infinitely large N_e , but they have much more power to set lower bounds for the range of N_e that is consistent with the data. Together, the demographic and genetic estimates constrain (bracket) plausible values of N_e/N in SBT to a much smaller range than would be possible using either method by itself.

The demographic analyses accounted for several factors that are rarely considered in estimating effective size in species with overlapping generations: skip breeding, persistent differences in reproductive success, and empirical data for ϕ . We estimate that skip breeding in SBT substantially reduces N_b but only slightly increases N_e , and thus does not have an appreciable effect on the N_e/N ratio. Our analyses show that

substantial and persistent individual differences in reproductive success can reduce N_e and N_e/N . However, differences in fecundity at age in SBT based on empirical data are not large enough to appreciably reduce N_e , even if they persist throughout an individual's adult life span.

The largest uncertainty regarding the N_e/N ratio in SBT is the value of ϕ . Minimum values of ϕ computed from observed variation in fecundity at age are barely above 1.0 and have little effect on N_e . Using these minimal estimates of ϕ and other life history parameters reported for SBT, we estimate that the upper bound for the effective size/census size ratio for SBT is relatively high ($0.5 < N_e/N < 1$). An important factor contributing to this result is delayed age at maturity, which increases generation length and hence N_e (refer to Eq. 1).

We consider the empirical ϕ estimates minimal because they do not account for other factors that might contribute to individual differences in reproductive success. Lacking any empirical data regarding these other potential factors, we evaluated consequences of assuming a range of possible fixed values of ϕ . We show that N_e/N for SBT could reach the tiny range ($\leq 10^{-3}$) only if ϕ is very large ($\sim 10^4$; fig. S1); this in turn would require a rather extreme form of SRS (21). The genetic data, which provide independent estimates of N_b/N and N_e/N , are particularly informative regarding uncertainty in ϕ ; they also provide insights into some of the less well-studied aspects of SBT biology. If ϕ were as large even as 50 in SBT, N_b would be reduced to $\sim 1.8 \times 10^4$ (Fig. 2 and table S3). This is below the lower 95% confidence bounds for the combined (across years) genetic estimates of N_b (Fig. 3). Furthermore, 1.8×10^4 is comparable to the smaller of the simulated effective sizes, and when we simulated populations with an effective size of 2×10^4 , the resulting distribution of estimates did not match the empirical genetic estimates of effective size (Fig. 4).

We cannot rule out values of ϕ in the range of 10 or so, which (after accounting for skip breeding) would produce $N_e \approx 8 \times 10^5$ and $N_e/N \approx 0.4$. These estimates would be consistent with empirically and theoretically derived N_e/N ratios for a large number of species (2, 3). The combined demographic and genetic results thus suggest that ϕ in SBT cannot be large enough to produce tiny N_e/N ratios comparable to those reported in the literature for some other highly fecund marine species. Similarly, if persistent differences in reproductive success were a substantial factor for SBT, the consequences should be reflected in the genetic estimates, but we do not find such evidence. We therefore conclude that the N_e/N ratio in SBT is above 0.1 and perhaps about 0.5.

It is important to emphasize that our results for SBT do not rule out SRS and tiny N_e/N ratios as potentially important factors for other species. However, it is noteworthy that two of the life history features commonly associated with SRS (broadcast spawning and very high fecundity) are also characteristics of SBT. Thus, our results demonstrate that SRS and very low N_e/N ratios are not an inevitable consequence of these life history traits.

Caveats

We collected genetic data used in this study from five consecutive years of juvenile and adult samples, which nevertheless represent only a fraction of one generation for SBT. We cannot rule out the possibility that extreme examples of SRS occur occasionally in SBT. However, if these events were common, they should be detectable as a signal of elevated LD, which decays only gradually over a period of several generations, and we did not find evidence for high LD.

The LD method is subject to potential bias due to both age structure and physical linkage of markers. Detailed life history information for SBT allowed us to make a quantitative adjustment to single-cohort estimates

of N_b (see Materials and Methods for details) (25). Effects of mixed-age samples on estimates of N_e are not as well understood, so that adjustment should be considered only approximate. The bias adjustment for physical linkage reflects the expected fraction of pairs of loci that are on the same chromosome or linkage group, which in turn depends on the number of chromosomes (26). As the number of loci becomes large, the actual fraction of linked pairs of loci should converge on the expected fraction, and the adjustment should become more precise. In studies like this one with at most a few dozen loci, the actual fraction of linked loci might deviate from the expected fraction, making the bias adjustment less reliable. However, we found no evidence for strong physical linkage in SBT (figs. S3 and S4). Overall, the combined effect of the two bias adjustments we implemented had little net effect (+4%) on genetic estimates of N_b . Combined adjustments were larger for N_e because both potential biases are in the same direction. However, 6 of the 10 genetic N_e estimates were already infinitely large before any adjustments; thus, overall, these adjustments had no appreciable effect on order-of-magnitude conclusions about effective size/census size ratios in SBT.

The AgeNe model (18) used for demographic estimates of effective size assumes stable age structure and constant population size, which are unlikely to be strictly true in any natural population. The CKMR study estimated a nonsignificant decline in adult SBT abundance over the period 2002–2010 (16). Previous work (18, 25) has shown that AgeNe results are robust to random demographic variation, and a similar model (27) accurately estimates N_e if population size changes at a constant rate.

It is well known [for example, (24)] that because genetic methods for estimating contemporary effective size depend on signals that are proportional to $1/N_e$, these methods have difficulty distinguishing very large and infinite effective sizes, and we see some evidence of that in results for SBT. The distribution of genetic estimates of N_b and N_e was bimodal, with about half being infinitely large and the rest falling in the range 10^4 to 10^6 . This pattern is typical for scenarios where true N_e is very large and the amount of data (numbers of individuals and numbers of genetic markers) is insufficient to produce high precision for individual point estimates (21). Nevertheless, in this study, the combination of (i) large samples of individuals (average >1000 per year for both juveniles and adults), (ii) a relatively large number of highly variable genetic markers, and (iii) replication across five consecutive years produced a distribution of estimates that effectively constrains the range of plausible values for effective population size, particularly on the lower end.

Conservation implications

The high estimated N_e/N ratio in SBT is generally good news from a conservation standpoint. The species is considered overfished and Critically Endangered by the International Union for Conservation of Nature (28). If N_e/N for SBT were in the tiny range, the species could be at some genetic risk, even with estimated abundance of $>10^6$ adults. Our results indicate that N_e is also close to 10^6 , which indicates that effective size is not likely to be a limiting factor for recovery. Nevertheless, because the amount of genetic diversity a population can maintain (and its ability to respond to rapid environmental change) is strongly influenced by N_e , careful attention to both N_e/N ratios and the absolute effective size is important.

Our results also emphasize the reality that large samples of individuals are essential if one wants robust estimates of effective size in large populations. Although empirical estimates of N_b and N_e for our large samples were bimodal, the lowest point estimates, and almost all lower bounds of CIs, were greater than 10^4 (Figs. 3 and 4). In contrast, if true

N_e were 10^6 but only typical sample sizes of 50 to 100 individuals had been used, the expected result is that most of the finite estimates would have fallen in the low hundreds to low thousands (21). The large samples used in the SBT study thus constrained the “blind spot” in genetic estimates of large N_e to a relatively small range. Unfortunately, use of samples of 1000 individuals or more to estimate effective size in populations that are known or suspected to be large is not common [see (29) for an exception]. Those interested in obtaining robust empirical estimates of N_e/N in large populations should include large samples of individuals from multiple time periods into the experimental design. In addition, using a combination of life history and genetic data to estimate effective size provides more robust estimates than can be obtained from either method by itself.

The SBT CKMR study began in 2006, and the battery of microsatellite loci used was sufficient to reliably identify parent-offspring pairs. In the past decade, orders-of-magnitude increases have been made in speed and cost-effectiveness of DNA sequencing, and it is now easy to assay many thousands of single-nucleotide polymorphism (SNP) markers, even for non-model species. This technological breakthrough now makes it feasible to expand the CKMR methodology to include reliable identification of siblings (30). In addition to providing increased precision for estimating abundance, this also opens up the possibility of adding the sibship method for estimating effective size (31) to the genetic toolbox for estimating N_e in large populations.

MATERIALS AND METHODS

Experimental design

Juveniles were sampled in association with a commercial harvest near Port Lincoln, South Australia, where immature fish are captured and raised in net pens before marketing. This fishery captures 2- to 4-year-olds that are distinguishable by size, and we used individual lengths to restrict our collections each year to single cohorts of age 3 fish. Adults were sampled from landings in a long-line fishery in Indonesia, where mixed-age adults are harvested. The current analyses used the same 5 years of samples used for the CKMR estimates of abundance (Table 1; juvenile, $S = 1316$ to 1625 per year; total = 7251 ; adult, $S = 212$ to 1466 per year; total = 5626). Each juvenile and adult sample was used to provide independent genetic estimates of effective size, and weighted harmonic means (with weights proportional to effective degrees of freedom) were used to obtain overall (across years) estimates for the two types of samples.

Population demography

Extensive geographic sampling has not produced any evidence of stock structure within SBT (32, 33). We therefore assumed that SBT comprise a single, isolated, randomly mating population. The CKMR study (16) reported abundance estimates in terms of biomass of age 10+ fish, whereas for our purposes, we want the number of adults age 8 and older. For the years 2002–2010, the mean estimated number of age 8 SBT recruits was 4.54×10^5 (23). Assuming an adult survival rate of 0.77 per year and a maximum longevity of 30 years (table S1), constant recruitment at this rate would produce a population of $N = 1.97 \times 10^6$ adults; hence, this is the value we used for the denominator in the N_e/N ratio.

Calculation of relative age-specific fecundity (b_x) involved two steps. First, on average, older fish are larger, and larger fish are more fecund, leading to higher fecundity with age in both sexes (Fig. 1). Second, larger females produce more eggs per kilo of body weight. There is no evidence that the same phenomenon occurs in males. Accordingly,

relative fecundity for males was assumed to be proportional to weight at age, while relative fecundity for females was proportional to the product of weight at age and per-kilo production of eggs. Because juvenile survival is poorly known for SBT, fecundity was expressed in terms of production of offspring that survive to age at maturity ($\alpha = 8$ years), and b_x was scaled to values required to produce a population of constant adult census size (N), given the modeled survival rates. Ignoring juvenile mortality affects both effective size and census size but not their ratio, which is of primary interest here. Empirical data for ϕ_x are rarely available, and that was also the case here. Empirical data on variance of fecundity at age (table S2) provided a means of calculating a minimum bound for ϕ_x , as described in detail in Supplementary Methods.

The model underlying AgeNe (18) assumes that reproduction and survival are independent across time periods (reproduction does not affect subsequent survival or reproduction). SBT violate this in at least two ways. First, in analyzing the number of years between parent-offspring pair matches in SBT, Bravington et al. (23) found evidence for every-other-year spawning for young (age 8 to 12) SBT of both sexes, but not for older fish; presumably, this occurs because energetic costs of reproduction are high. Consequences of skip breeding for N_e and N_b were evaluated using the model developed by Waples and Antao (22). On the basis of the skip-breeding data (23), we reduced the number of available spawners each year by 50% for ages 8 to 12.

Second, individuals that are unusually large (or small) at an early age are also likely to have positive (or negative) residuals for size at later ages, which would lead to positive correlations in realized fecundity over time. To evaluate consequences of persistent individual differences for SBT, we modeled lifetime reproductive success for the N_1 individuals born into the same cohort. Individuals in the cohort survived randomly each year with probability s_x and on reaching age x produced an average of b_x offspring, as specified in table S1. As a point of reference, random reproductive success in each time period among individuals in the cohort was modeled by a Poisson process with $\phi_x = 1$ (equivalent to assuming that all individuals have the same expected fecundity). If larger fish of the same age have higher expected fecundity, ϕ_x will be >1 , leading to overdispersed variance in reproductive success. From table S2, the median coefficient of variation of age-specific fecundity related to variation in fecundity at age is $CV(b_x) = 0.1$. This provides a measure of overdispersion, which we used to calculate ϕ_x for use in AgeNe as described above and in Supplementary Methods. However, the AgeNe model assumes that these variations in expected fecundity are random and uncorrelated across years. To model persistent individual differences, for each individual in a newborn cohort, we selected a random normal deviate (z) and found its associated probability (rnorm and pnorm functions in R). This characterized the relative expected reproductive success for that individual at every age throughout its life. For example, for a female SBT with $z = 1.3$, $pnorm(1.3) = 0.9$, indicating that this individual's expected reproductive success would be in the 90th percentile every year it survived to reproduce. At age 20, SBT females on average produce $b_{20} = 1.595$ offspring that survive to recruitment (table S1). Assuming a $CV(b_x) = 0.1$ implies $SD(b_{20}) = 0.16$, and the 90th percentile of the normal distribution with mean = 1.595 and SD = 0.16 is 1.8. Thus, our consistently "above average" fish had expected reproductive success at age 20 of 1.8 offspring that survive to age at recruitment, about 13% above the mean. This value of 1.8 was then used as the parameter for a random Poisson draw to determine how many offspring that individual actually produced in that time period. We kept track of lifetime reproductive output for all members of the cohort and used that information to calculate V_{K_x} and N_e using Eq. 1.

Genetic data

The genetic analyses used 5 years of samples of juveniles and adults scored for up to 27 microsatellite loci [see (23) for detailed information about the genetic methodology]. In the CKMR study (16), several additional loci were added after the first phase of sampling to boost power to detect parent-offspring pairs. Only ambiguous juveniles sampled in the early phase were subsequently scored for the additional loci. In addition, in all samples, loci scored as missing were re-run only for individuals for which the additional information might have affected parent-offspring status. As a consequence, the distribution of missing data was somewhat uneven across the data set. After dropping two loci not scored in a substantial fraction of individuals, and then dropping individuals missing data for more than 10 loci (fig. S2), we had a data set with 25 loci and 12,877 individuals (5626 adults and 7251 juveniles; Table 1 and table S4).

Genetic estimates of effective size

We used the single-sample LD method to estimate effective size. The LD method is based on random associations of alleles at different gene loci; these occur in all finite populations and can be quantified by the squared correlation coefficient r^2 , which is inversely related to N_e (34). We calculated mean r^2 and estimated effective size using the program LDNe (35), as implemented in NeEstimator V2.1 (36). The juvenile samples are from single cohorts and can be used to estimate N_b (37), while the mixed-age adult samples can be used to estimate N_e (25). The LD method estimates effective size in the parents of the individuals sampled (37), so these effective size estimates can be compared directly with estimates of adult census size obtained through CKMR.

LD estimates were computed using two different criteria for screening out rare alleles: $P_{\text{crit}} = 0.02$ (all alleles with frequencies <0.02 are omitted) and $P_{\text{crit}} = 0.01$. $P_{\text{crit}} = 0.02$ was recommended as a generally good way to balance effects on precision and bias (24), but we also considered the more lenient $P_{\text{crit}} = 0.01$ because of the large sample sizes (more than 1000 individuals/year, except for 1 year of adult sampling). The two P_{crit} values provided a total of 10 point estimates of N_e and N_b , along with combined estimates computed as weighted harmonic means across all 5 years. Two of the 25 loci (D569 and D573) had relatively high ($>10\%$) estimated frequencies of null alleles (16), so in an additional sensitivity analysis, we repeated the effective size estimates after dropping them. As estimates using 23 versus 25 loci did not differ appreciably (Fig. 3), we focused on the 25 locus analyses in Results. Also, because estimates using $P_{\text{crit}} = 0.01$ used the most data, we considered them the most robust.

We adjusted the raw genetic effective size estimates in two ways to account for age structure and physical linkage. If some pairs of loci are physically linked, LD and r^2 will be higher than expected from drift alone, which will downwardly bias estimated N_e unless an adjustment is made. Physical linkage can be accounted for if the recombination rate for each pair of loci is known (34, 38) or if all loci can be mapped to their chromosomes, but detailed linkage information is not available for SBT. Instead, we applied a generic correction factor based on the ln (haploid) number of chromosomes (Chr), which determines the fraction of locus pairs expected to be in each linkage category (26)

$$\hat{N}_{e(\text{adj})} = \frac{\hat{N}_{e(\text{raw})}}{0.098 + 0.219 \times \ln(\text{Chr})} \quad (3)$$

The haploid chromosome number for SBT is 23 (39), so we calculated bias-adjusted estimates of effective size as the raw estimate divided by

$0.098 + 0.219 \times \ln(23) = 0.785$. The net effect of these adjustments was to increase the point estimates of N_e and N_b (and their CIs) by $1/0.785 = 27\%$ to account for physical linkage.

As described in Supplementary Methods, we also examined the SBT genetic data for evidence that certain pairs of loci consistently produced relatively high r^2 values; if so, that could lead to larger bias than was accounted for by the adjustment in Eq. 3. No such evidence was found (see fig. S3 and S4).

Age structure affects single-cohort and mixed-age samples differently (25). The juvenile samples are from single cohorts and thus provide information most directly relevant to N_b , but with some influence from background N_e per generation. If an estimate of the N_b/N_e ratio is available, age structure can be accounted for by dividing the raw estimate by the factor $1.26 - 0.323 \times N_b/N_e$ (25). For this purpose, we used the demographic estimate of $N_b/N_e = 0.121$ obtained for constant $\phi = 10$ (table S3). The age-structure adjustment thus became $\hat{N}_{b(\text{adj})} = \hat{N}_{b(\text{raw})} / (1.26 - 0.323 \times N_b/N_e) = \hat{N}_{b(\text{raw})} / 1.22$, which translated to a reduction of 18% for each point estimate. Mixed-age adult samples are more relevant to N_e per generation, but they are expected to be downwardly biased because of mixture LD created by combining progeny from multiple cohorts with slightly different allele frequencies. The maximum number of cohorts that could have been included in each adult sample is the adult life span (23 breeding cycles, from age 8 to 30, inclusive), which is 1.7 times the generation length of 13.3 years. Previous work (25) has shown that adult LD estimates of N_e were biased downward by about 25% for iteroparous species for which the ratio of adult life span to generation length is in the range 1.5 to 2. Therefore, we adjusted each raw adult estimate upward by dividing it by 0.75 to account for age-structure effects. The net effect of these two adjustments was an increase of +4% for each raw point estimate of N_b and an increase of +69% for each raw point estimate of N_e . We also considered two other genetic estimators of effective size—one based on the incidence of siblings, and the other based on temporal changes in allele frequency—but neither proved suitable for the SBT data sets (see Supplementary Methods for details).

To provide some context for interpreting the LD estimates of effective size, we modified the simulation model described by Waples (21) to tune it to mimic the amount of data available for SBT. The number of pairwise comparisons of alleles used in the LD analyses using $P_{\text{crit}} = 0.01$ ranged from $n = 62,000$ to 66,000, which is the number that would be produced by all pairwise comparisons of about 350 to 360 loci with two alleles each. Except for the first year of adult samples, the remaining collections of juveniles and adults all included 1160 to 1625 individuals. Therefore, we simulated genotypes for 350 unlinked, diallelic SNP gene loci in discrete-generation populations of known effective size and estimated N_e using samples of $S = 1500$ individuals. We modeled two effective sizes: $N_e = 5 \times 10^5$ and 2×10^4 , each using 500 replicates. (Results for simulations using $N_e = 10^6$ were qualitatively similar to those for $N_e = 5 \times 10^5$ and are not shown.) After initialization, the population was allowed to reproduce randomly for eight generations before sampling.

Statistical analysis

CIs for genetic estimates of N_b and N_e were calculated using NeEstimator V2.1, which incorporates an improved jackknife method (40) that accounts for pseudoreplication due to both physical linkage and overlapping pairs of loci. Distributions of \hat{N}_e for data simulated under the two effective sizes were compared with empirical distributions for \hat{N}_e and \hat{N}_b using the nonparametric Kolmogorov-Smirnov test (ks.test function in R). Infinite estimates were coded as 10^9 for these comparisons.

SUPPLEMENTARY MATERIALS

Supplementary material for this article is available at <http://advances.sciencemag.org/cgi/content/full/4/7/eaar7759/DC1>

Supplementary Methods

Table S1. Life table for SBT, using age at maturity $\alpha = 8$ and maximum age $\omega = 30$.

Table S2. Illustration of how to calculate effects of variation in fecundity at age on ϕ_x (the ratio of variance to mean reproductive success in 1 year for individuals of age x).

Table S3. Estimates of effective size in SBT.

Table S4. Microsatellite loci used in the analyses reported here.

Fig. S1. Demographic estimates of the N_e/N ratio for SBT as a function of $\phi_x = V_{\text{tot}}/b_x$, which is the ratio of the variance to the mean reproductive success in one time period for individuals of age x .

Fig. S2. Distribution of missing loci across individuals.

Fig. S3. Evaluation of evidence for physical linkage.

Fig. S4. Distribution of statistics related to physical linkage for randomized data.

References (41–48)

REFERENCES AND NOTES

1. B. Charlesworth, Fundamental concepts in genetics: Effective population size and patterns of molecular evolution and variation. *Nat. Rev. Genet.* **10**, 195–205 (2009).
2. R. Frankham, Effective population size/adult population size ratios in wildlife: A review. *Genet. Res.* **66**, 95–107 (1995).
3. F. P. Palstra, D. J. Fraser, Effective/census population size ratio estimation: A compendium and appraisal. *Ecol. Evol.* **2**, 2357–2365 (2012).
4. L. Nunney, The influence of mating system and overlapping generations on effective population size. *Evolution* **47**, 1329–1341 (1993).
5. L. Nunney, D. R. Elam, Estimating the effective population size of conserved populations. *Conserv. Biol.* **8**, 175–184 (1994).
6. A. M. Lee, S. Engen, B.-E. Saether, The influence of persistent individual differences and age at maturity on effective population size. *Proc. Biol. Sci.* **278**, 3303–3312 (2011).
7. R. S. Waples, G. Luikart, J. R. Faulkner, D. A. Tallmon, Simple life-history traits explain key effective population size ratios across diverse taxa. *Proc. Biol. Sci.* **280**, 20131339 (2013).
8. W. R. Ardren, A. R. Kapuscinski, Demographic and genetic estimates of effective population size (N_e) reveals genetic compensation in steelhead trout. *Mol. Ecol.* **12**, 35–49 (2002).
9. E. V. Saarinen, J. D. Austin, J. C. Daniels, Genetic estimates of contemporary effective population size in an endangered butterfly indicate a possible role for genetic compensation. *Evol. Appl.* **3**, 28–39 (2010).
10. A. Kuparinen, J. A. Hutchings, R. S. Waples, Harvest-induced evolution and effective population size. *Evol. Appl.* **9**, 658–672 (2016).
11. A. M. Myhre, S. Engen, B.-E. Saether, Effective size of density-dependent populations in fluctuating environments. *Evolution* **70**, 2431–2446 (2016).
12. D. Hedgecock, Does variance in reproductive success limit effective population size of marine organisms? in *Genetics and Evolution of Aquatic Organisms*, A. R. Beaumont, Ed. (Chapman & Hall, 1994), pp. 122–134.
13. D. Hedgecock, A. I. Pudovkin, Sweepstakes reproductive success in highly fecund marine fish and shellfish: A review and commentary. *Bull. Mar. Sci.* **87**, 971–1002 (2011).
14. L. Hauser, G. R. Carvalho, Paradigm shifts in marine fisheries genetics: Ugly hypotheses slain by beautiful facts. *Fish. Fish.* **9**, 333–362 (2008).
15. H.-S. Niwa, K. Nashida, T. Yanagimoto, Allelic inflation in depleted fish populations with low recruitment. *ICES J. Mar. Sci.* **74**, 1639–1647 (2017).
16. M. V. Bravington, P. M. Grewe, C. R. Davies, Absolute abundance of southern bluefin tuna estimated by close-kin mark-recapture. *Nat. Commun.* **7**, 13162 (2016).
17. H. Caswell, *Matrix Population Models: Construction, Analysis and Interpretation* (Sinauer Associates, 2001).
18. R. S. Waples, C. Do, J. Chopelet, Calculating N_e and N_e/N in age-structured populations: A hybrid Felsenstein-Hill approach. *Ecology* **92**, 1513–1522 (2011).
19. W. G. Hill, Effective size of populations with overlapping generations. *Theor. Popul. Biol.* **3**, 278–289 (1972).
20. A. Caballero, Developments in the prediction of effective population size. *Heredity* **73**, 657–679 (1994).
21. R. S. Waples, Tiny estimates of the N_e/N ratio in marine fishes: Are they real? *J. Fish Biol.* **89**, 2479–2504 (2016).
22. R. S. Waples, T. Antao, Intermittent breeding and constraints on litter size: Consequences for effective population size per generation (N_g) and per reproductive cycle (N_b). *Evolution* **68**, 1722–1734 (2014).
23. M. V. Bravington, P. G. Grewe, C. R. Davies, “Fishery-independent estimate of spawning biomass of Southern Bluefin Tuna through identification of close-kin using genetic markers” (FRDC Report 2007/034, Australia, 2014).
24. R. S. Waples, C. Do, Linkage disequilibrium estimates of contemporary N_e using highly variable genetic markers: A largely untapped resource for applied conservation and evolution. *Evol. Appl.* **3**, 244–262 (2010).

25. R. S. Waples, T. Antao, G. Luikart, Effects of overlapping generations on linkage disequilibrium estimates of effective population size. *Genetics* **197**, 769–780 (2014).
26. R. K. Waples, W. A. Larson, R. S. Waples, Estimating contemporary effective population size in non-model species using linkage disequilibrium across thousands of loci. *Heredity* **117**, 233–240 (2016).
27. J. Felsenstein, Inbreeding and variance effective numbers in populations with overlapping generations. *Genetics* **68**, 581–597 (1971).
28. B. Collette, S.-K. Chang, A. Di Natale, W. Fox, M. Juan Jorda, N. Miyabe, R. Nelson, Y. Uozumi, S. Wang, *Thunnus maccoyii*. *The IUCN Red List of Threatened Species 2011* (2011); <http://dx.doi.org/10.2305/IUCN.UK.2011-2.RLTS.T21858A9328286.en>.
29. G. M. Macbeth, D. Broderick, R. C. Buckworth, J. R. Ovenden, Linkage disequilibrium estimation of effective population size with immigrants from divergent populations: A case study on spanish mackerel (*Scomberomorus commerson*). *G3* **3**, 709–717 (2013).
30. B. M. Hillary, M. V. Bravington, T. A. Patterson, P. Grewe, R. Bradford, P. Feutry, R. Gunasekera, V. Peddemors, J. Werry, M. P. Francis, C. A. J. Duffy, B. D. Bruce, Genetic relatedness reveals total population size of white sharks in eastern Australia and New Zealand. *Sci. Rep.* **8**, 2661 (2018).
31. J. Wang, A new method for estimating effective population sizes from a single sample of multilocus genotypes. *Mol. Ecol.* **18**, 2148–2164 (2009).
32. P. M. Grewe, N. G. Elliott, B. H. Innes, R. D. Ward, Genetic population structure of southern bluefin tuna (*Thunnus maccoyii*). *Mar. Biol.* **127**, 555–561 (1997).
33. J. H. Farley, J. P. Eveson, T. L. O. Davis, R. Andamari, C. H. Proctor, B. Nugraha, C. R. Davies, Demographic structure, sex ratio and growth rates of southern bluefin tuna (*Thunnus maccoyii*) on the spawning ground. *PLOS ONE* **9**, e96392 (2014).
34. W. G. Hill, Estimation of effective population size from data on linkage disequilibrium. *Genet. Res.* **38**, 209–216 (1981).
35. R. S. Waples, C. Do, LDNe: A program for estimating effective population size from data on linkage disequilibrium. *Mol. Ecol. Resour.* **8**, 753–756 (2008).
36. C. Do, R. S. Waples, D. Peel, G. M. Macbeth, B. J. Tillet, J. R. Ovenden, NeEstimator V2: Re-implementation of software for the estimation of contemporary effective population size (N_e) from genetic data. *Mol. Ecol. Resour.* **14**, 209–214 (2014).
37. R. S. Waples, Genetic estimates of contemporary effective population size: To what time periods do the estimates apply? *Mol. Ecol.* **14**, 3335–3352 (2005).
38. C. M. Hollenbeck, D. S. Portnoy, J. R. Gold, A method for detecting recent changes in contemporary effective population size from linkage disequilibrium at linked and unlinked loci. *Heredity* **117**, 207–216 (2016).
39. P. A. Bain, R. G. Hutchinson, A. B. Marks, M. St. J. Crane, K. A. Schuller, Establishment of a continuous cell line from southern bluefin tuna (*Thunnus maccoyii*). *Aquaculture* **376–379**, 59–63 (2013).
40. A. T. Jones, J. R. Ovenden, Y.-G. Wang, Improved confidence intervals for the linkage disequilibrium method for estimating effective population size. *Heredity* **117**, 217–223 (2016).
41. J. H. Farley, T. L. O. Davis, M. V. Bravington, R. Andamari, C. R. Davies, Spawning dynamics and size related trends in reproductive parameters of southern bluefin tuna, *Thunnus maccoyii*. *PLOS ONE* **10**, e0125744 (2015).
42. R. M. Hillary, A. P. Preece, C. R. Davies, *Updates Required for New Data Sources and Reconditioning of the CCSBT OM* (Canberra, Australia, 2017).
43. R. S. Waples, Evaluating the effect of stage-specific survivorship on the N_e/N ratio. *Mol. Ecol.* **11**, 1029–1037 (2002).
44. J. Wang, A comparison of single-sample estimators of effective population sizes from genetic marker data. *Mol. Ecol.* **25**, 4692–4711 (2016).
45. M. V. Bravington, J. P. Eveson, P. M. Grewe, C. R. Davies, “Close-Kin Mark-Recapture with Parent-Offspring and Half-Sibling Pairs: Update on genotyping, kin-finding and model development” (Scientific Committee Report CCSBT-ESC/1709/12, Hobart, Tasmania, Australia, 2017).
46. R. S. Waples, M. Yokota, Temporal estimates of effective population size in species with overlapping generations. *Genetics* **175**, 219–233 (2007).
47. P. E. Jorde, Allele frequency covariance among cohorts and its use in estimating effective size of age-structured populations. *Mol. Ecol. Resour.* **12**, 476–480 (2012).
48. P. E. Jorde, N. Ryman, Temporal allele frequency change and estimation of effective size in populations with overlapping generations. *Genetics* **139**, 1077–1090 (1995).

Acknowledgments: We thank O. Berry and five anonymous reviewers for valuable comments on the manuscript. **Funding:** Tenure of R.S.W. in Hobart was supported by a Frohlich Fellowship from CSIRO and by an International Science Fellowship from the National Marine Fisheries Service. **Author contributions:** P.M.G. and R.S.W. conceived and designed the research. P.M.G. collected the genetic data. M.W.B. led the CKMR study that provided the estimate of adult abundance. R.H. and M.W.B. compiled the life history data. R.S.W. conducted the analyses and wrote the manuscript. All authors read and edited the manuscript. **Competing interests:** The authors declare that they have no competing interests. **Data and materials availability:** Data are available from the Dryad Digital Repository (<https://doi.org/10.5061/dryad.46g67n8>). All other data not presented in the manuscript have been previously published. All data needed to evaluate the conclusions in the paper are present in the paper and/or the Supplementary Materials. Additional data related to this paper may be requested from the authors.

Submitted 15 December 2017

Accepted 11 June 2018

Published 18 July 2018

10.1126/sciadv.aar7759

Citation: R. S. Waples, P. M. Grewe, M. W. Bravington, R. Hillary, P. Feutry, Robust estimates of a high N_e/N ratio in a top marine predator, southern bluefin tuna. *Sci. Adv.* **4**, eaar7759 (2018).

Robust estimates of a high N_e/N ratio in a top marine predator, southern bluefin tuna

Robin S. Waples, Peter M. Grewe, Mark W. Bravington, Richard Hillary and Pierre Feutry

Sci Adv 4 (7), eaar7759.
DOI: 10.1126/sciadv.aar7759

ARTICLE TOOLS

<http://advances.sciencemag.org/content/4/7/eaar7759>

SUPPLEMENTARY MATERIALS

<http://advances.sciencemag.org/content/suppl/2018/07/16/4.7.eaar7759.DC1>

REFERENCES

This article cites 42 articles, 4 of which you can access for free
<http://advances.sciencemag.org/content/4/7/eaar7759#BIBL>

PERMISSIONS

<http://www.sciencemag.org/help/reprints-and-permissions>

Use of this article is subject to the [Terms of Service](#)

Science Advances (ISSN 2375-2548) is published by the American Association for the Advancement of Science, 1200 New York Avenue NW, Washington, DC 20005. The title *Science Advances* is a registered trademark of AAAS.

Copyright © 2018 The Authors, some rights reserved; exclusive licensee American Association for the Advancement of Science. No claim to original U.S. Government Works. Distributed under a Creative Commons Attribution NonCommercial License 4.0 (CC BY-NC).